MOLECULAR ONCOLOGY 9 (2015) 1348–1358

available at www.sciencedirect.com

ScienceDirect

www.elsevier.com/locate/molonc

Potent anti-tumor response by targeting B cell maturation antigen (BCMA) in a mouse model of multiple myeloma

Felix Oden[a,*], *Stephen F. Marino*[b,**], *Janko Brand*[b], *Susanne Scheu*[a], *Cathleen Kriegel*[a], *Daniel Olal*[b], *Anna Takvorian*[c], *Jörg Westermann*[c], *Buket Yilmaz*[d], *Michael Hinz*[d], *Oliver Daumke*[b], *Uta E. Höpken*[a], *Gerd Müller*[a], *Martin Lipp*[a,***]

[a]*Max-Delbrück-Center of Molecular Medicine (MDC), Department of Tumor Genetics and Immunogenetics, Robert-Rössle-Strasse 10, 13125 Berlin, Germany*
[b]*Max-Delbrück-Center of Molecular Medicine, Crystallography, Robert-Rössle-Strasse 10, 13125 Berlin, Germany*
[c]*Charité University Medicine Berlin, Campus Virchow-Klinikum, Department of Hematology, Oncology and Tumor Immunology, Augustenburger Platz 1, 13353 Berlin, Germany*
[d]*Max-Delbrück-Center for Molecular Medicine (MDC), Department of Signal Transduction in Tumor Cells, Robert-Rössle-Strasse 10, 13125 Berlin, Germany*

ARTICLE INFO

Article history:
Received 21 November 2014
Received in revised form
23 March 2015
Accepted 24 March 2015
Available online 31 March 2015

Keywords:
B cell maturation antigen (BCMA)
Immunotherapy
Multiple myeloma
Monoclonal antibody
Xenograft mouse model
High resolution X-ray structure

ABSTRACT

Multiple myeloma (MM) is an aggressive incurable plasma cell malignancy with a median life expectancy of less than seven years. Antibody-based therapies have demonstrated substantial clinical benefit for patients with hematological malignancies, particular in B cell Non-Hodgkin's lymphoma. The lack of immunotherapies specifically targeting MM cells led us to develop a human-mouse chimeric antibody directed against the B cell maturation antigen (BCMA), which is almost exclusively expressed on plasma cells and multiple myeloma cells. The high affinity antibody blocks the binding of the native ligands APRIL and BAFF to BCMA. This finding is rationalized by the high resolution crystal structure of the Fab fragment in complex with the extracellular domain of BCMA. Most importantly, the antibody effectively depletes MM cells *in vitro* and *in vivo* and substantially prolongs tumor-free survival under therapeutic conditions in a xenograft mouse model. A BCMA-antibody-based therapy is therefore a promising option for the effective treatment of multiple myeloma and autoimmune diseases.

1. Introduction

Multiple myeloma (MM) is an aggressive neoplasm resulting from the malignant transformation of plasma cells (PCs) and their precursors (Palumbo and Anderson, 2011; Raab et al., 2009). High dose chemotherapy followed by autologous stem cell transplantation has prolonged survival after diagnosis by approximately 4–5 years (Hideshima and Anderson, 2002;

* *Corresponding author*. Tel.: +49 30 9406 3830; fax: +49 30 9406 3814.
** *Corresponding author*. Tel.: +49 30 9406 3280; fax: +49 30 9406 3814.
*** *Corresponding author*. Tel.: +49 30 9406 2886; fax: +49 30 9406 3884.
E-mail addresses: felix.oden@mdc-berlin.de (F. Oden), stephen.marino@mdc-berlin.de (S.F. Marino), mlipp@mdc-berlin.de (M. Lipp).
http://dx.doi.org/10.1016/j.molonc.2015.03.010

Munshi and Anderson, 2013; Palumbo and Anderson, 2011; Raab et al., 2009; Richardson et al., 2003; Yang and Yi, 2011). The recent introduction of anti-angiogenic drugs like thalidomide or lenalidomide and the proteasome inhibitor bortezomib into the clinic has improved the median survival of MM patients to 5–7 years (Hideshima and Anderson, 2002; Munshi and Anderson, 2013; Palumbo and Anderson, 2011; Raab et al., 2009; Richardson et al., 2003; Yang and Yi, 2011). However, despite these advances, MM is still incurable in most patients. Therefore, the need for new drugs for efficient clearance of the malignant cells remains.

During the past two decades monoclonal antibodies have increasingly been used for the treatment of hematological malignancies. For example, treatment with Rituximab, a monoclonal antibody (mAb) against CD20, in combination with chemotherapy, has dramatically improved the long-term survival of patients suffering from Non-Hodgkin's Lymphoma (Cheson and Leonard, 2008). Accordingly, mAbs targeting cell surface molecules expressed on MM cells like CD38, CD70 or CD138 are currently in preclinical development or in early phase clinical trials. Strategies interfering with the tumor growth-promoting bone marrow (BM) environment by targeting B cell growth factors such as IL-6, APRIL, and/or BAFF have also reached the clinic (Munshi and Anderson, 2013; Rossi et al., 2009; Tai and Anderson, 2011; Yang and Yi, 2011). However, there are as yet no approved antibody-based therapies for MM. In addition, the epitopes of mAbs in clinical development are not exclusively present on MM cells. CD38, for instance, is also expressed on activated B and T cells (Malavasi et al., 2008) and CD138 is present on epithelial cells (Inki and Jalkanen, 1996). Therefore, we generated an antibody against the B cell maturation antigen (BCMA), which is almost exclusively expressed on plasma blasts and plasma cells but is absent from naive, germinal center and memory B cells (Benson et al., 2008; Darce et al., 2007; Good et al., 2009). BCMA is a receptor for APRIL and BAFF and is known to be important for the survival of long-lived PCs in the BM (O'Connor et al., 2004). Previous findings by Ryan et al. (2007) showed that antibodies and antibody-drug conjugates (ADC) directed against BCMA blocked APRIL binding and led to an efficient depletion of MM cells *in vitro* (O'Connor et al., 2004). It was not shown, however, whether such antibodies could target MM cells *in vivo*. Here, we report the development of a new chimeric antibody which binds with high affinity to the ligand binding site of BCMA. This antibody blocks BCMA signaling, efficiently depletes MM cells *in vitro* and *in vivo* and substantially increases tumor-free survival in a mouse model of MM. Our high resolution structure of the Fab in complex with the extracellular domain of human BCMA provides a detailed picture of the antibody's epitope and will help to facilitate humanization and sequence optimization.

2. Methods

2.1. BCMA expression and purification

Human BCMA (residues 1–54) was expressed from the pGEX6p-1 vector (GE Healthcare) as an N-terminal glutathione-S-transferase (GST) fusion followed by a PreScission cleavage site. Proteins were expressed in *Escherichia coli* host strain Rosetta2-BL21-DE3, and bacteria were cultured in TB medium at 37 °C to an OD_{600} of 0.5 followed by induction with 60 μM Isopropyl β-D-1-thiogalactopyranoside (IPTG) and temperature shift to 18 °C for overnight expression. Cells were resuspended in buffer A (50 mM HEPES/NaOH, pH 7.5, 500 mM NaCl 1 μM DNase (Roche), 500 μM Pefabloc (Roth)) and disrupted in a microfluidizer (Microfluidics). Cleared lysates (95,000 g, 1 h, 4 °C) were incubated with Benzonase (Novagen) for 30 min at 4 °C prior to application to a GSH column (Clontech). Protein was eluted with buffer A containing 20 mM GSH. Fractions containing BCMA were incubated with His_6-tagged PreScission protease overnight at 4 °C. Non-cleaved BCMA and free GST were removed by a second application to a GSH column. The flow-through and four column volumes of washing buffer A were collected and concentrated using 5 kDa mw cut-off concentrators (Amicon). Finally, BCMA was subjected to size exclusion chromatography on a Superdex200 column (GE) in buffer containing 20 mM HEPES/NaOH (pH 7.5), 300 mM NaCl. Fractions containing BCMA were pooled, concentrated and flash-frozen in liquid nitrogen.

2.2. Generation of hybridoma J22.9

C57BL/6 wild type mice were immunized with the human BCMA extracellular domain (residues 1–54) N-terminally fused to GST. Using standard hybridoma technology (Yokoyama, 2006), splenocytes of immunized mice were fused to ×63-Ag 8.653 murine myeloma cells.

2.3. Production and purification of the chimeric antibodies J22.9-xi and isoAb

Variable regions of the light and heavy chain of the mouse hybridoma J22.9 were amplified and cloned upstream of the human kappa and IgG1 constant domain genes, respectively (Tiller et al., 2009). The chimeric J22.9-xi antibody was produced by transient cotransfection of the 2 chains in 293-6E cells using the pTT vector system (Durocher et al., 2002). In brief: 293-6E cells at 1.7×10^6 cells/ml in F17 medium were transfected using polyethyleneimine with a 1:2.5 DNA:PEI mixture of plasmid DNA carrying the heavy and light chain genes with N-terminal secretion signal peptides, at a final concentration of 1 μg/ml culture. Two days after transfection, cells were fed with 100% of the transfection volume of Freestyle F17 medium containing 1% tryptone N1 (Organo Technie). At day 7, cells were harvested by centrifugation and the filtered (0.45 μm) culture medium was passed over 3.5 ml UNOshpere SUPrA Protein A affinity medium (Bio-Rad). The column was washed with 10 ml PBS and antibody eluted by addition of 20 mM sodium acetate, 150 mM NaCl, pH 3.5. 2 ml fractions were collected directly into tubes containing 100 μl 1 M HEPES, pH 7.5 for neutralization. The final yield of full length IgG was approximately 40 mg/l culture.

The isotype control antibody (isoAb) comprising the J22.9-xi heavy chain and a random chimeric kappa light chain was produced in parallel with J22.9-xi. This antibody did not bind to BCMA in either ELISA or flow cytometry.

The N-linked oligosaccharide chains at Asn297 of J22.9-xi were removed enzymatically using N-Glycosidase F (PNGase F) (NEB). 10 mg of J22.9-xi were incubated with 15,000 units PNGase F in 500 μl PBS (pH 7.4) for 36 h at 37 °C followed by buffer exchange into sterile PBS.

2.4. Generation of Fab and Fab:BCMA complexes

$(Fab)_2$ fragments were generated from full length J22.9-xi by incubation with pepsin. Per mg J22.9-xi, 30 μg Pepsin was added in 50 mM sodium acetate, pH 3.5. Incubation at 37 °C for 2.5 h was sufficient to completely digest the F_c and pepsin was inactivated by exchange over a PD-10 column into PBS. The reduction of the $(Fab)_2$ fragments to individual Fabs was accomplished in PBS by addition of 2-Mercaptoethylamine to 50 mM in the presence of 5 mM EDTA. After incubation for 90 min at 37 °C, the reduced cysteines were blocked by alkylation with 500 μM iodoacetamide for 30 min followed by buffer exchange into PBS. Fab fragments were combined with 1.5 molar equivalents of purified BCMA and the complexes isolated by size exclusion chromatography on a Superdex75 16/60 column. Fractions were analyzed on 4–12% SDS polyacrylamide gels and fractions containing both Fab and BCMA were pooled and concentrated for crystallization trials.

2.5. Crystallization of Fab:BCMA complexes

Concentrated complexes were supplemented with 0.5 molar equivalents of pure BCMA to ensure saturation and were subjected to crystallization screening. Initial Fab:BCMA crystallization conditions were identified from commercial screens in 96-well sitting drop format plates using a Gryphon pipetting robot (200 nl drops) and optimized in 24-well plates in hanging drops (3 μl). Crystals were grown by mixing 1 μl of the complex at a concentration of 8 mg/ml with 2 μl of 21% PEG 3350, 0.1 M BisTris pH 6.5 and 5 mM $CuCl_2$ at 20 °C. Crystals appeared after 3 days as clusters of thin plates and attained their final size (0.2–0.3 mm) within approximately 7 days. Clusters were separated and individual plates were flash-frozen in liquid nitrogen in mother liquor with 20% glycerol as cryoprotectant. Complete diffraction data from 42 to 1.74 Å resolution were collected from a single crystal at BL14.1 at BESSY II, Berlin. Data were processed using the XDS program suite (Kabsch, 2010), and the structure was solved by molecular replacement with MOLREP (Vagin and Teplyakov, 2010), using the structure of Efalizumab (pdb i.d. 3EO9) as the search model. The model was built with COOT (Emsley et al., 2010) and iteratively refined using PHENIX (Adams et al., 2010). The final model comprises two heavy chains (residues 1–133, and 139–220 in chain A and residues 1–135 and 141–220 in chain H), two light chains (residues 1–213 in chain B and residues 1–213 in chain L) and two BCMA molecules (residues 6–41 in chain F and residues 8–37 in chain K). 98.4% of all residues are in the most favored regions of the Ramachandran plot and no residue in the disallowed regions, as analyzed by MolProbity (Chen et al., 2010). Figures were prepared using the PyMOL Molecular Graphics System, Version 1.5.0.4 (Schrödinger, LLC), domain superpositions were performed with COOT (Emsley et al., 2010) and the schematic interaction diagrams were generated using PDBSum (Laskowski et al., 1997).

2.6. Luciferase-based in vitro cytotoxicity assay

In order to test the cytotoxic potential of J22.9-xi, a luciferase-based cytotoxicity assay was established using luciferase transduced MM.1S-Luc cells. In this assay, only bioluminescence of living cells is detected, whereas luciferase released by dead cells is non-functional due to insufficient ATP in the medium (Fu et al., 2010). Peripheral blood mononuclear cells (PBMCs) from five healthy donors were isolated from freshly obtained filter buffy coats as described previously (Meyer et al., 2005). After erythrocyte lysis, PBMCs were washed and adjusted by dilution in RPMI/10% FCS w/o phenol red to 1×10^7 cells/ml. 5×10^4 MM.1S-Luc cells in 50 μl RPMI were plated in microtiter plates. Ten minutes prior to addition of 100 μl PBMCs, MM.1S-Luc cells were incubated with J22.9-xi, J22.9-xi-N-glycan or isoAb serial dilutions in sample volumes of 200 μl. Before incubation at 37 °C with 5% CO_2, microtiter plates were centrifuged (300 g) for 2 min at room temperature (RT). Control wells for complete lysis were treated with 1% Triton X instead of antibody. After 4 h, 25 μl of PBS with luciferin (250 ng/ml) were applied to each well, and bioluminescence was measured (Tecan). Cytotoxicity relative to isoAb was calculated according to the following formula:

$$100 - [\text{value}(J22.9 - xi) - \text{value}(\text{total lysis})]/[\text{value}(\text{isoAb}) - \text{value}(\text{total lysis})] * 100.$$

2.7. In vivo animal studies

Female SCID-Beige and NOD-SCID common gamma chain mice (NSG) lacking functional B, T and NK cells were used. The NSG strain additionally supports engraftments through transgenic expression of the cytokines IL-3, CSF2 and KITLG, boosting tumor growth. Experiments were performed on 6–8 week old mice. All animal studies were performed according to institutional and state guidelines, under specific pathogen-free conditions.

The xenograft model of MM was induced by tail vein injection of 1×10^7 MM.1S-Luc cells at day zero. Tumor challenged animals developed hind limb paralysis within 6 (NSG) to 8 (SCID-Beige) weeks – the experimental endpoint of survival.

For efficacy studies, antibodies were administered intraperitoneally (i.p.) twice a week or on 5 consecutive days starting at day zero. J22.9-xi was given in doses of 2, 20 or 200 μg per injection; for isoAb, 200 μg/injection was used. Bioluminescence of MM.1S-Luc cells was measured weekly after i.p. injection of 150 μg luciferin (Biosynth) using an IVIS Spectrum (Caliper LifeSciences). Total flux values of 3 control mice animals were either subtracted from each measurement or are shown in the graphs. Images were analyzed with Living Image 3.0 software (Caliper LifeScience).

To treat established tumors, antibody therapy was started 5 or 12 days after tumor challenge, and 200 μg isoAb or J22.9-xi per injection administered twice weekly for a period of 6 weeks.

2.8. Supplemental methods

The methodological details of ELISA, EMSA, western blot and flow cytometry analyses as well as information about cell

lines and the statistical analyses are given in the supplemental data section.

3. Results

3.1. Strong and specific binding of J22.9-xi to BCMA

BCMA, a member of the tumor necrosis factor receptor superfamily, represents a potential target for therapeutic intervention of multiple myeloma. We immunized mice with a purified BCMA extracellular domain and used standard hybridoma technology to isolate mAbs. Binding of mAb J22.9 to BCMA was confirmed by ELISA (data not shown) and, subsequently, its light and heavy chain variable regions were fused to the human Igκ and IgG1 constant domains, respectively, to produce the chimeric antibody J22.9-xi. J22.9-xi binds BCMA in ELISA (Figure 1A). It also detects BCMA on the human MM cell lines MM.1S, NCI–H929, OPM-2, and RPMI-8226, as shown by flow cytometry (Figure 1B), but does not bind to BCMA-negative Jurkat cells (Figure 1C). The affinity, determined using surface plasmon resonance, was 54 pM (Figure 1D), making J22.9-xi the highest affinity ligand known for BCMA. Flow cytometry analyses revealed that cells from bone marrow of MM patients were detectable using an anti-CD138 antibody and J22.9-xi (Figure 1E).

3.2. J22.9-xi blocks ligand interaction and APRIL-induced NF-κB activation

BCMA activates canonical and/or non-canonical nuclear factor-κB (NF-κB) pathways (Rickert et al., 2011) and triggers signals important for survival of MM and PCs *in vivo* through interaction with APRIL and/or BAFF (Mackay et al., 2003). We could demonstrate that J22.9-xi interferes with ligand binding to BCMA, whereas no blocking effect was observed with our control antibody isoAb (Figure 2A). Likewise, J22.9-xi interfered with APRIL-induced phosphorylation of the T-loop activation domain in IKK and subsequent IκBα degradation (Figure 2B) leading to a reduced NF-κB DNA-binding activity in NCI–H929 cells (Figure 2C). Addition of J22.9-xi alone activated neither the canonical nor the non-canonical NF-κB pathway, as analyzed by IKK phosphorylation, IκB degradation and NF-κB2 p100 processing, in all tested cell lines (Figure S1A-C). High levels of processed NF-κB B2 p52 indicate that multiple myeloma derived cell lines already display constitutive non-canonical NF-κB signaling (Figure S1A and B).

We next analyzed whether antibody treatment affected JNK or PI3K/AKT signaling. MM cells have been shown to display constitutive AKT activation (Hsu et al., 2001; Ramakrishnan et al., 2012). Accordingly, we observed strong and constitutive AKT phosphorylation in NCI–H929 cells, which was not further increased by platelet derived growth factor (PDGF) treatment. Application of J22.9-xi did not interfere with AKT activation (Figure S1D). In addition, we observed that J22.9-xi induces JNK phosphorylation (Figure S1E). However, treatment with the control antibody isoAb resulted in the same or even stronger JNK activation, indicating that antibody treatment causes a BCMA-independent JNK activation (Figure S1E). In line with these observations, J22.9-xi showed no effect on the viability of NCI–H929 cells (Figure S1F). In summary, our pathway analyses indicate a specific inhibitory function of J22.9-xi for BCMA-mediated NF-κB activation.

3.3. J22.9-xi recognizes the physiological BCMA epitope

To understand these observations on a molecular level, we determined the crystal structure of the J22.9-xi Fab fragment in complex with the purified 54 amino acid residue BCMA extracellular domain to a maximal resolution of 1.89 Å (Figure 3A, Table S1). Two identical BCMA-Fab complexes were present in the asymmetric unit. In the following, we describe the complex with the better resolved BCMA molecule. High quality electron density was observable for residues 6–41 of BCMA, including very well defined side chains in the binding interface around the conserved DxL motif (Figure S2A).

Direct contacts in the 740 Å^2 interface are primarily hydrophobic, with the bulk occurring between BCMA and residues from all three complementarity determining regions (CDRs) of the J22.9-xi light chain (Figure 3C, Figure S2B,C). Although the heavy chain contributes only six residues in total, at least one residue from each CDR is involved in the interaction. In addition, the interface comprises numerous water-mediated contacts (Figure S2D). The BCMA epitope surface features the DxL motif (Gordon et al., 2003), which protrudes into a central cavity of the antigen binding site (Figure 3A–C).

Interestingly, the interaction with J22.9-xi covers most of the BCMA epitope also targeted by APRIL (Hymowitz et al., 2005) (10 of 14 residues) and BAFF (Liu et al., 2003) (10 of 16 residues) (Figure 3B). As with APRIL and BAFF, the DxL motif is completely surrounded by the ligand in the J22.9-xi Fab structure. This provides clear rationalization of the blocking effect of J22.9-xi seen with BAFF and APRIL (Figure 2). The overall conformation of BCMA in all three structures is very similar, with a root mean square deviation (rmsd) of the C-alpha atoms of 1.4 Å between the J22.9-xi and APRIL complexes and 1.5 Å between the J22.9-xi and BAFF complexes (Figure 3D). Strikingly, the respective C-alpha rmsds for the J22.9-xi BCMA binding epitope (residues 13–30) are only 0.98 and 0.88 Å. This indicates that J22.9-xi recognizes a functional BCMA signaling conformation.

3.4. Strong cytotoxic effect of J22.9-xi depends largely on glycosylation

In order to test the cytotoxic potential of J22.9-xi, a luciferase-based cytotoxicity assay was established using luciferase transduced MM.1S-Luc cells. Lysis of MM.1S cells reached 18–35% in the presence of 125 ng/ml J22.9-xi and increased to 56% at 1 μg/ml (Figure 4A). BCMA-negative Jurkat cells were not depleted by J22.9-xi (Figure S3A).

Productive interaction of IgG1 with Fcγ receptors (FcγR) on effector cells or with the C1q protein of the complement cascade is dependent on glycosylation of the antibody at position 297 in the heavy chain constant region (Jefferis et al., 1998; Nezlin and Ghetie, 2004; Shields et al., 2001). Deglycosylation of J22.9-xi with PNGase F (J22.9-xi-N-glycan) was verified by a shift in the apparent molecular mass of the heavy chain on an SDS gel (Figure S3B). Although deglycosylation had no

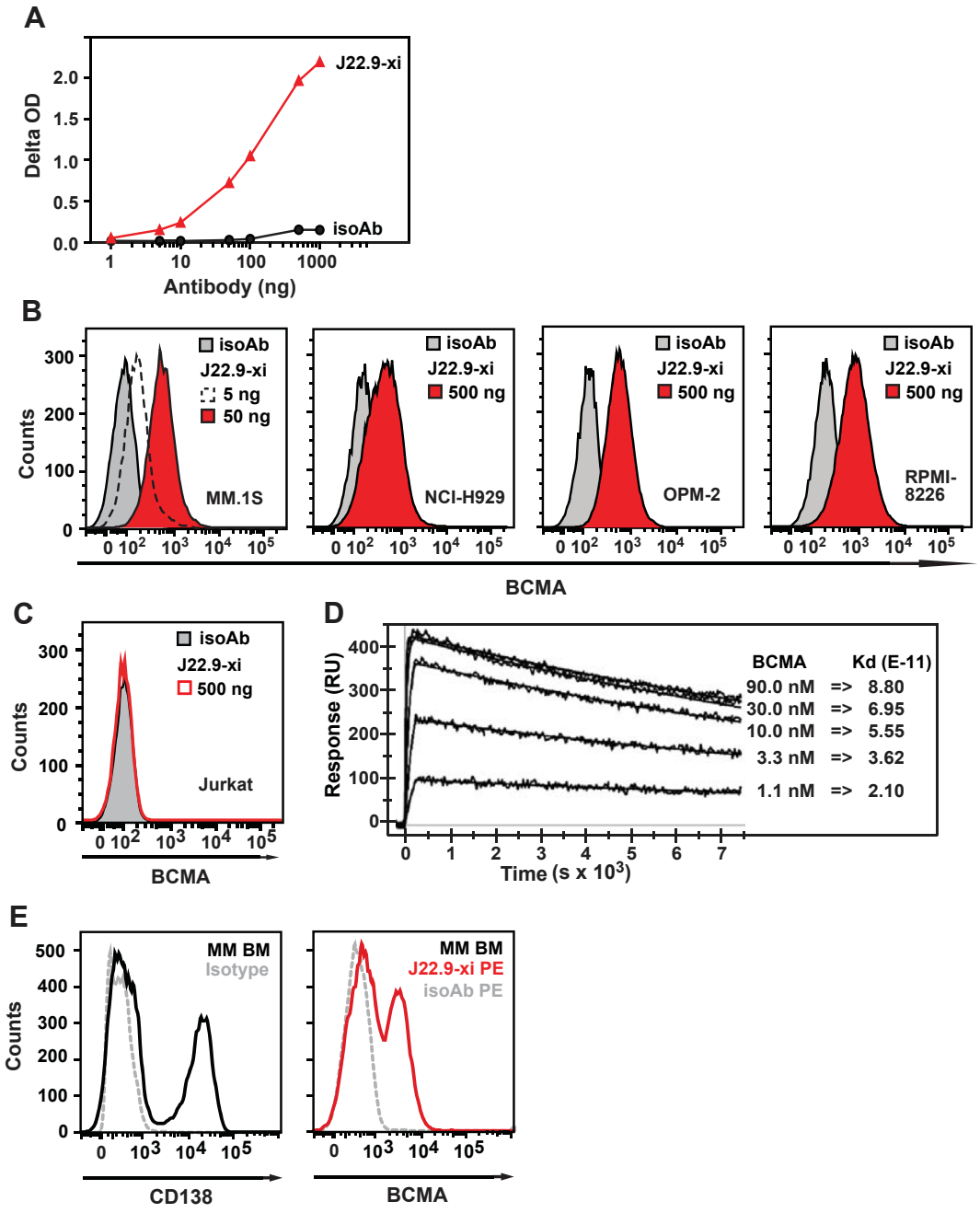

Figure 1 – J22.9-xi is a high affinity antibody for human BCMA. A) ELISA on BCMA-coated microtiter plates and B) flow cytometry analyses using BCMA-positive MM.1S, NCI–H929, OPM-2, and RPMI-8226 cell lines. Chimeric antibodies were detected using an HRP-conjugated or PE-conjugated goat anti-human secondary antibody, respectively. Experiments were performed in sextuplicate (A) and triplicate (B), respectively. C) No binding of J22.9-xi to BCMA-negative Jurkat cells is detectable using flow cytometry. Shown is one of two independent experiments. D) Binding affinity was determined from surface plasmon resonance measurements with indicated concentrations of BCMA. Shown is one out of three independent experiments. E) Flow cytometry analysis of myeloma cells in the BM of an MM patient stained with a standard diagnostic antibody against CD138 and with J22.9-xi. Dotted lines represent isotype control staining. Shown is one representative BM sample of five analyzed samples from MM patients.

impact on the ability of J22.9-xi-N-glycan to bind to BCMA (Figure 4B), the antibody-mediated cytotoxicity decreased to below 8% (Figure 4A). This observation reveals that cell lysis is primarily due to antibody-dependent cellular cytotoxicity (ADCC). By using serum instead of PBMCs, we also determined the complement-dependent cytotoxicity (CDC) of J22.9-xi and J22.9-xi-N-glycan. As expected, approximately 45% of MM.1S-Luc cells were depleted after 1 h of incubation with J22.9-xi but less than 10% CDC was seen for J22.9-xi-N-glycan (Figure S3C). These results indicate that glycosylation of J22.9-xi is required for efficient recruitment of effector cells and activation of the complement system.

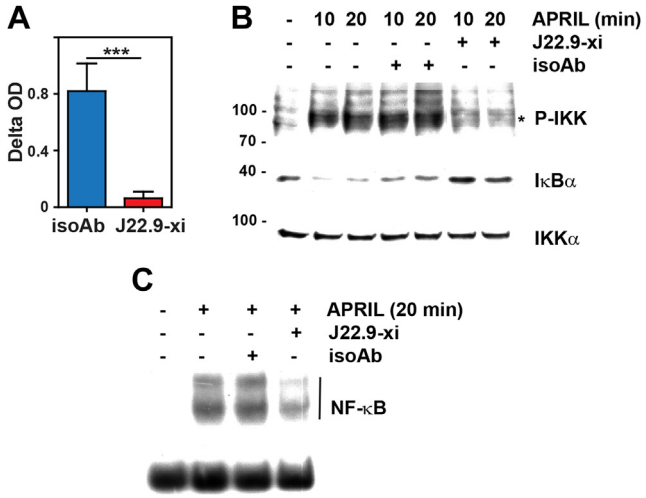

Figure 2 – J22.9-xi blocks BAFF and interferes with NF-κB activation. A) J22.9-xi blocks the interaction of BAFF with BCMA adsorbed onto microtiter plates. Error bars indicate the standard error of the mean (SEM) of triplicates (*$P < 0.001$, t-test); shown is one out of three independent experiments. B) NCI–H929 cells were pre-incubated with 10 μg J22-Xi or control-antibody for 10 min and subsequently stimulated with 500 ng APRIL for 10 or 20 min, as indicated. Cells were lysed with whole cell lysis buffer and analyzed by immunoblotting. Signals representing Phospho-IKK are indicated by an asterisk. The IKKα band serves as an internal loading control, since expression levels do not change in a stimulus dependent manner. Shown is one out of two independent experiments. C) Whole cell extracts of NCI cells treated as in (B) were used to monitor NF-κB activation (EMSA). The lower band is a result of unspecific DNA binding activity within the protein extract and serves as a loading control.**

3.5. *J22.9-xi decreases tumor burden and prolongs survival significantly*

We next tested the cytotoxic activity of J22.9-xi *in vivo* using a xenograft tumor model. After tumor cell challenge, mice were randomly divided into 5 groups. Groups one ($n = 4$), two and three (each $n = 5$) were treated with 200, 20 and 2 μg of J22.9-xi per injection (i.p.), which equates to approximately 10, 1 and 0.1 mg/kg body weight, respectively. To determine whether blocking of BCMA upon binding of J22.9-xi has any impact on tumor development, we administered J22.9-xi-N-glycan, which neither efficiently recruits effector cells nor activates the complement system, at 200 μg per injection to group 4 ($n = 6$). As control, group five ($n = 5$) was treated with 200 μg isoAb. Antibodies were administered i.p. for five succeeding days starting with the day of tumor challenge (Figure 5A). The tumor load of the isoAb treated controls increased steadily from week 2 forward, whereas tumor-derived bioluminescence was still not seen at day 44 in any of the groups receiving intact J22.9-xi (Figure 5B,E). Consistent with this finding, tumor development was significantly reduced in J22.9-xi treated mice (Figure 5C) and their survival time was nearly tripled (Figure 5D). Tumor growth in animals treated with J22.9-xi-N-glycan was decelerated (Figure 5B,C), and their mean lifespan was prolonged by 35% (Figure 5D), indicating that binding of J22.9-xi-N-glycan to BCMA alone has a negative impact on MM.1S-Luc cell survival *in vivo*. Interestingly, in short term cell culture experiments, neither APRIL nor J22.9-xi altered the high basal level of NF-κB activation in MM.1S cells (Figure S1B). To better mimic the *in vivo* environmental factors in our cell culture assays, we co-cultured MM.1S-Luc cells with the bone marrow stromal cell line M2-10B4 and treated these cultures either with isoAb or J22.9-xi. Independent of the treatment, no changes in the viability of MM.1S-Luc cells were observed (Figure S1G).

In a second experiment, we used NSG mice which developed hind limb paralysis approximately 25% faster than SCID-Beige mice. We consequently chose a repetitive antibody administration of 10 mg/kg per injection of either J22.9-xi ($n = 6$) or isoAB ($n = 5$) twice weekly for a period of 6 weeks, starting with the day of tumor challenge (Figure S4A). Mice injected with J22.9-xi showed strongly decelerated tumor growth for the first 5 weeks (Figure S4B) and a significant reduction in the overall tumor load compared with the isoAb group (Figure S4C). The effectiveness of the antibody was reflected in the median survival, which was extended in J22.9-xi treated mice by 55% (Figure S4D).

In both studies, all animals responded to J22.9-xi treatment and showed a strikingly decreased tumor burden and increased lifespan, demonstrating the *in vivo* potency of J22.9-xi.

3.6. *J22.9-xi substantially increases lifespan in model therapeutic settings*

We next intended to determine the *in vivo* efficacy of J22.9-xi in a therapeutic approach by delaying the start of antibody treatment to day 5 after tumor cell challenge (Figure 6A). Xenografted SCID-Beige mice received 200 μg per injection of either isoAb ($n = 6$) or J22.9-xi ($n = 5$) twice per week. While there was no detectable tumor-derived bioluminescence before day 35 in the group receiving J22.9-xi, a steady increase in tumor load was seen in animals receiving isoAb (Figure 6B,E), resulting in a significantly increased overall tumor load (Figure 6C). Tumor challenged mice treated with isoAb survived on average 56 days, while the median lifespan of mice receiving J22.9-xi was more than tripled (Figure 6D).

Using the NSG mouse strain and starting the J22.9-xi antibody treatment at day 12 after tumor challenge (Figure S5A) extended the lifespan of mice by about 18% compared to mice receiving isoAb (Figure S5B). These two studies confirm the efficacy of J22.9-xi *in vivo* and underscore the benefit of the chimeric antibody J22.9-xi in these therapeutic models.

4. Discussion

Multiple myeloma is an incurable plasma cell malignancy, and much effort has been devoted over the years to identifying reagents that specifically deplete MM cells (Hideshima and Anderson, 2002; Schwartz and Vozniak, 2008; Yang and Yi, 2011). BCMA has for some time been recognized as potential target for the treatment of MM, since its expression is restricted to terminally differentiated cells of the B cell lineage

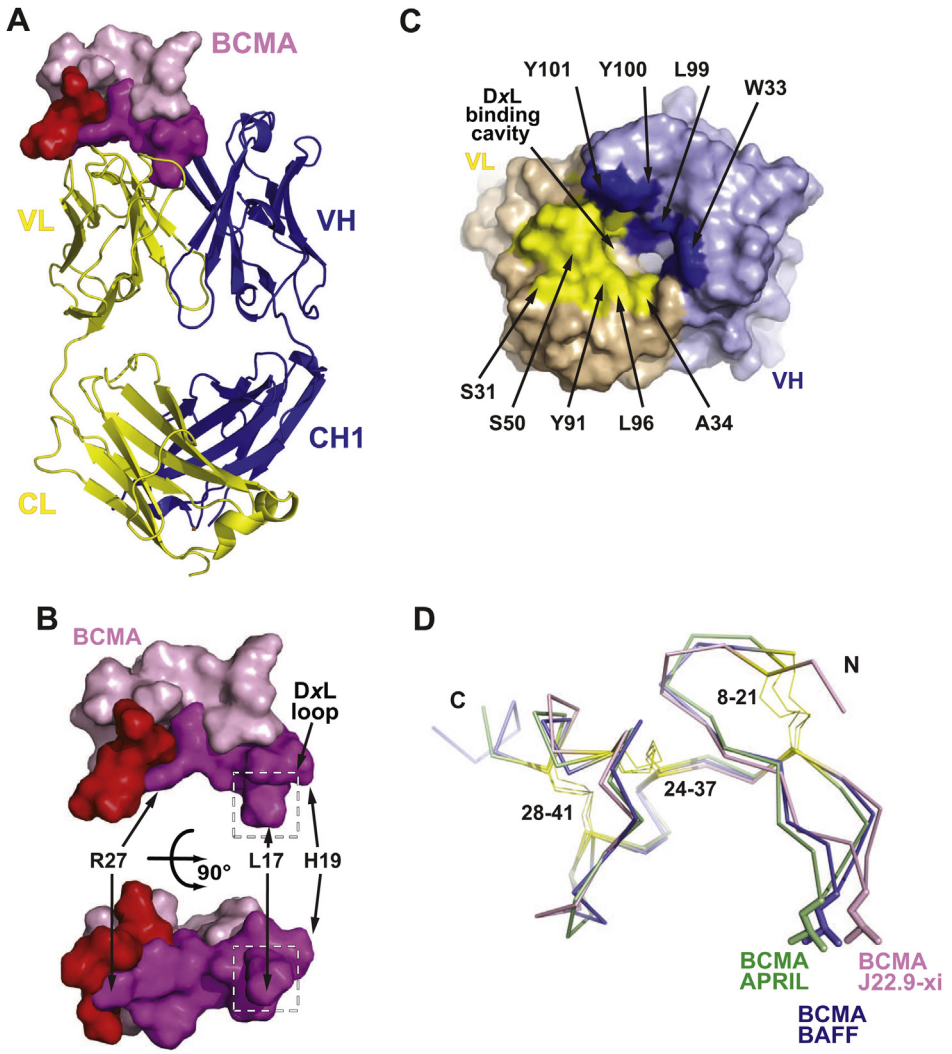

Figure 3 – J22.9-xi binds the same BCMA epitope as APRIL and BAFF. A) Structure of the J22.9-xi Fab:BCMA complex. The heavy (blue) and light (yellow) chains of the Fab fragment are shown in ribbon-type and BCMA in surface representation. B) J22.9-xi recognizes the same epitope as APRIL and BAFF. Orthogonal views of the BCMA binding face, with colors as in (A). Residues contacted by APRIL, BAFF and J22.9-xi are colored magenta and residues exclusively contacted by APRIL or BAFF are colored red. Leu17 of the D*x*L motif is at the apex of the protruding loop of BCMA that fits into a cavity in J22.9-xi. Interface residues Arg27 and His19 are shown for orientation. C) Surface view of the binding site in J22.9-xi, colored as in (A). Residues contacting BCMA are labelled. D) Backbone superposition of BCMA from three crystal structures. BCMA from the complex with APRIL (green, pdb i.d. 1XU2), from the complex with BAFF (blue, pdb i.d. 1OQD) and from the J22.9-xi complex (magenta). The side chain of Leu17 from the D*x*L motif is explicitly shown and the N- and C-termini are indicated, as are the three disulphide bonds (yellow) and their respective residue numbers.

and it is important for the survival of long-lived, sessile PCs in the BM (Carpenter et al., 2013; O'Connor et al., 2004; Ryan et al., 2007). Importantly, BCMA is highly expressed on malignant PCs including MM and plasma cell leukemia (PCL), which is more aggressive than MM and constitutes around 4% of all PC disorders. Some patients responding favorably to allogenic haematopoetic stem cell transplantation develop graft versus tumor response based on anti-BCMA antibodies in the serum (Bellucci et al., 2005). Consistent with its function on PCs, ligand binding to BCMA has been shown to modulate the growth and survival of MM cells (Novak et al., 2004). Furthermore, antibodies and ADCs directed against BCMA effectively recognize MM cell lines *in vitro* and induce their depletion in cytotoxicity studies (Novak et al., 2004). This prompted the development of a chimeric antigen receptor T cell (CART) which efficiently depletes solid xenograft MM tumors (Novak et al., 2004). While these studies provided proof of principle that targeting BCMA is a viable approach for MM treatment, using CARTs in clinical applications is connected with several safety issues (Xu and Tang, 2014). During the submission of the present manuscript, another study reported an afucosylated auristatin F ADC directed against BCMA with potent *in vitro* and *in vivo* anti-multiple myeloma activity (Tai et al., 2014), validating the potential of targeting BCMA for the treatment of MM in humans.

In this study, we describe a BCMA-specific monoclonal antibody that efficiently blocks binding of APRIL and BAFF to BCMA and rationalize these findings from the crystal structure

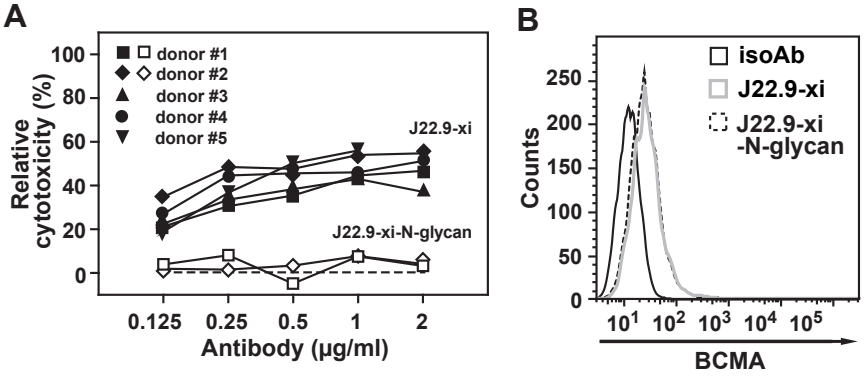

Figure 4 – J22.9-xi mediates strong cytotoxic effects *in vitro*. A) BCMA-positive MM.1S-Luc cells were mixed with unstimulated human PBMCs (from 5 donors (#1–#5)) at an effector to target ratio of 20:1 and incubated with the indicated concentrations of J22.9-xi for 4 h (filed symbols). Open symbols indicate cytotoxic activity of J22.9-xi-N-glycan when incubated with PBMCs from donor 1 or 2. Cytotoxicity was calculated relative to isoAb (dotted line) and subtracted from 100 using bioluminescence measurements of the living cells. B) No detectable difference in binding to MM.1S cells is observed between J22.9-xi and J22.9-xi-N-glycan using flow cytometry. Shown is one out of two independent experiments.

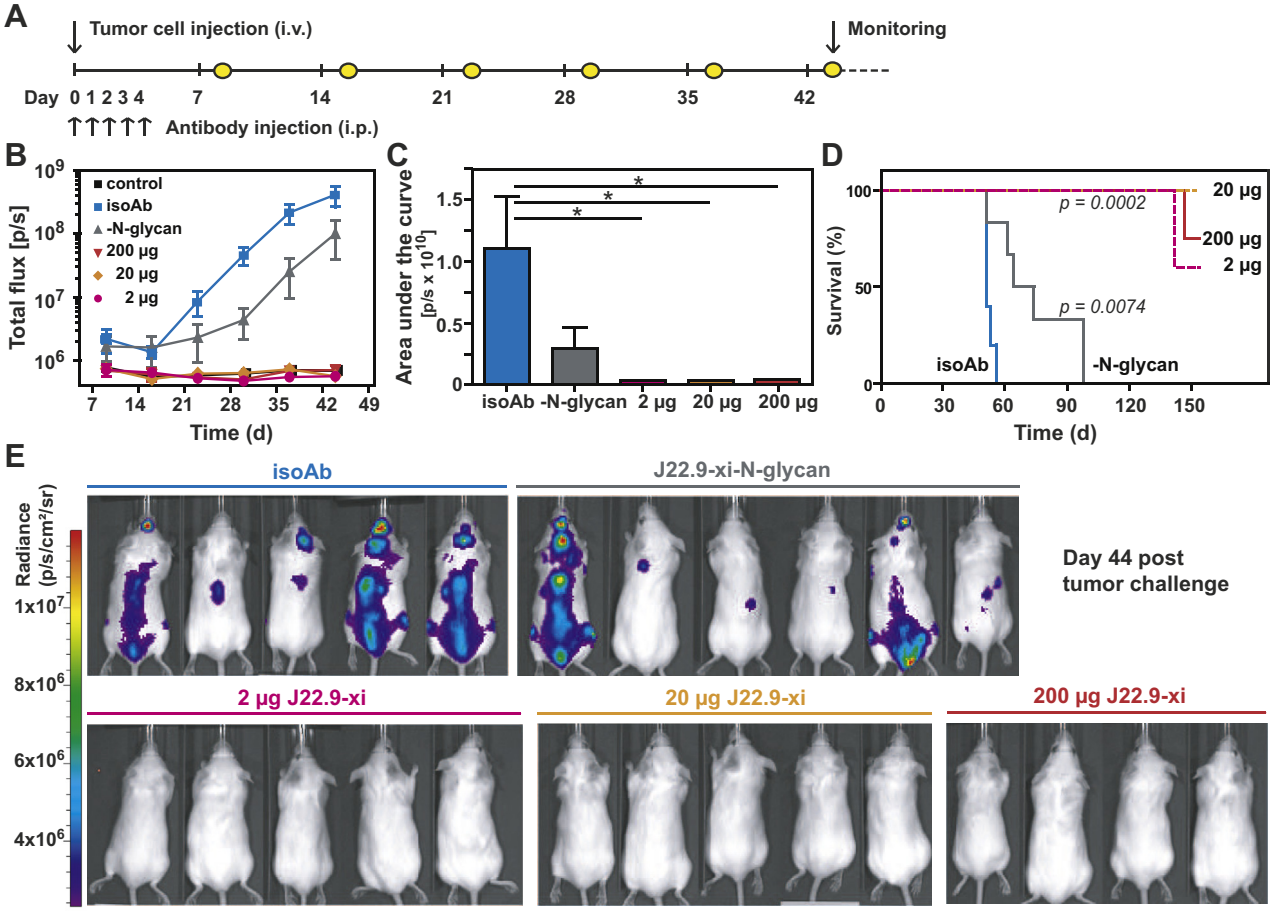

Figure 5 – J22.9-xi is effective against tumors in a xenografted mouse model. A) Experimental timeline: antibody treatment of xenografted SCID Beige mice for the first 5 days starting with the day of tumor cell challenge (1×10^7 cells/mouse). Open circles indicate days of bioluminescence measurements. B) Course of tumor growth in mice treated with 2 ($n = 5$), 20 ($n = 5$) or 200 µg ($n = 4$) of J22.9-xi or 200 µg of either isoAb ($n = 5$) or J22.9-xi-N-glycan ($n = 6$), and without tumor ($n = 3$; control). Background of bioluminescence was determined using NSG mice not challenged with MM.1S-Luc cells ($n = 3$; control). C) Tumor development over time, represented as area under curve of (B), between days 9 and 44. Mean of total flux from unchallenged mice was subtracted. Shown are the mean values with SEM (*$P < 0.05$, 2-tailed t-test). D) Survival of antibody-treated and control xenografted SCID Beige mice. The *P* values were calculated using the Log-rank (Mantel–Cox) Test. E) Distribution of MM.1S-Luc cells in the indicated groups at day 44 post tumor challenge; dorsal view.

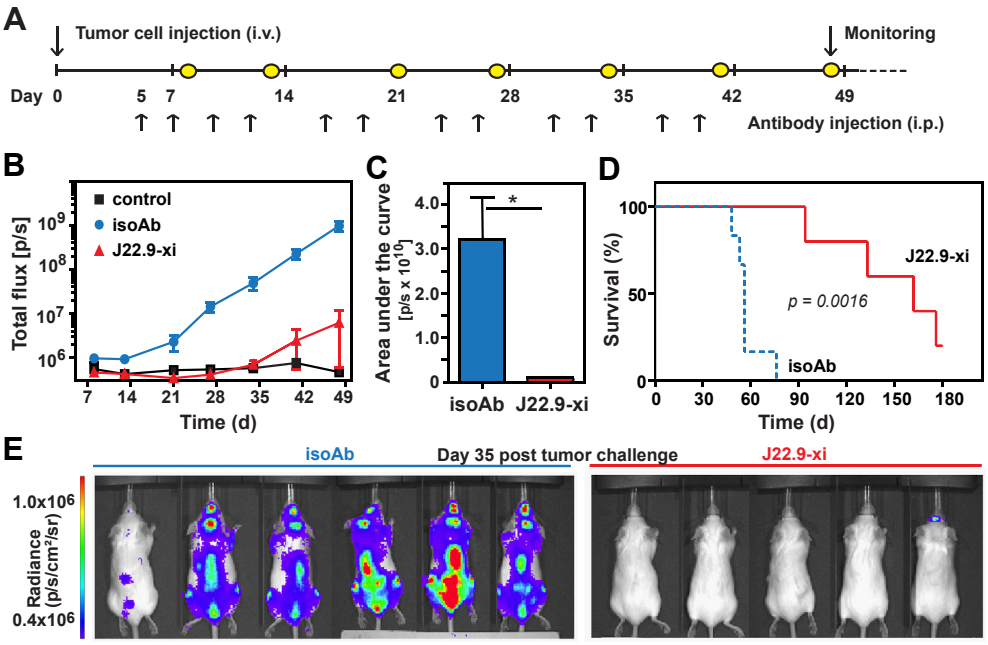

Figure 6 – J22.9-xi prolongs lifespan of SCID Beige mice in a therapeutic approach. A) Experimental timeline: antibody treatment twice a week starting at day 5 post tumor cell challenge (1×10^7 cells/mouse). Open circles indicate days of bioluminescence measurements. B) Tumor development over time with administration of 200 μg of J22.9-xi ($n = 5$) or isoAb ($n = 6$) twice weekly starting at day 5 after tumor challenge. Background of bioluminescence was determined using NSG mice not challenged with MM.1S-Luc cells ($n = 3$; control). C) Tumor development over time between day 9 and 48 of J22.9-xi and isoAb treated mice, represented as area under the curve of B). Mean of total flux of unchallenged mice was subtracted. Plotted are the mean values with SEM (*$P < 0.05$, 2-tailed t-test). D) Overall survival of J22.9-xi treated SCID Beige mice. The *P* value was calculated using the Log-rank (Mantel–Cox) Test. E) Distribution of MM.1S-Luc cells in the indicated groups at day 44 post tumor challenge; dorsal view.

of the Fab:BCMA complex. J22.9-xi binds the majority of the interaction surface contacted by the native ligands of BCMA, APRIL and BAFF, as determined from their respective crystal structures (Hymowitz et al., 2005; Liu et al., 2003). In addition, the affinity of J22.9-xi exceeds that of APRIL and BAFF by 300- and 30,000-fold (Bossen and Schneider, 2006), respectively. Signaling of BAFF and APRIL via BCMA is facilitated through NF-κB activation. Although J22.9-xi covers most of the epitopes of APRIL and BAFF, binding of J22.9-xi to MM.1S and NCI–H929 cells does not result in activation of canonical or further increase of non-canonical NF-κB signaling, but does abrogate APRIL-induced NF-κB activation in NCI–H929 cells. Due to the fact that signaling by BAFF and APRIL via BCMA is responsible for cell survival through up-regulation of anti-apoptotic Bcl-2 members such as Bcl-xL or Bcl-2 and Mcl-1 (Peperzak et al., 2013), the disruption of the ligand–receptor interaction should improve the therapeutic outcome in MM. This mode of action is already being exploited by use of Atacicept in clinical trials, mainly for the treatment of autoimmune disorders (Bracewell et al., 2009). Atacicept is a TACI-Ig fusion protein, which binds to APRIL and BAFF. However, it is not specific for MM or plasma cells, since mature B cells, which express the BAFF-receptor, also rely on the presence of BAFF (Jefferis et al., 1998; Nezlin and Ghetie, 2004).

The *in vitro* cytotoxicity assays revealed a strong and specific ADCC induction upon J22.9-xi binding to BCMA-positive cells. This may also be the main mode of action *in vivo*, as all the immune cells capable of ADCC, except NK cells, are still present in the mouse strains used in this work (Nimmerjahn and Ravetch, 2007). In all *in vivo* studies, we observed a substantial prolongation of median survival for J22.9-xi treated animals. We demonstrated that an initial boost-administration of this antibody over the first 5 successive days efficiently suppressed MM.1S-Luc tumor cell growth even at a dose as low as 0.1 mg/kg body weight per injection. This might be attributed to the high affinity of J22.9-xi to BCMA which hinders dissociation of the antibody from tumor cells, increasing its half-life. Independent of the dose, the lifespan of all mice receiving J22.9-xi was prolonged by more than 150%. Even NSG mice, in which xenograft survival is further supported through transgenic cytokines, showed a reduced overall tumor load and an extension of median survival by 55%. Surprisingly, treating mice with deglycosylated J22.9-xi, which is unable to induce meaningful ADCC or CDC (Jefferis et al., 1998; Nezlin and Ghetie, 2004), still extended the lifespan of xenografted mice by 35% compared to isoAb treated mice. Although we cannot exclude that the *in vivo* effect of J22.9-xi-N-glycan is based on background ADCC or CDC, this result suggests that binding of J22.9-xi and J22.9-xi-N-glycan to BCMA alone has a negative impact on tumor development. The non-canonical NF-κB pathway in MM.1S cells is constitutively active due to a biallelic deletion of the TRAF3 gene (Demchenko et al., 2010) and we show that activation is not further stimulated by addition of APRIL or BAFF. This observation indicates that blocking

the NF-κB pathway was not crucial for the depletion of tumors in our experimental setup. Consistent with this observation, we also saw no influence of the antibodies on cell viabilities in our *in vitro* assays with either the MM.1S or the NCI–H929 cell lines. Further studies need to clarify whether J22.9-xi-mediated BCMA inhibition interferes with NF-κB mediated signal transduction *in vivo*. In addition, BCMA might regulate other tumor-relevant signaling pathways.

To address the functionality of J22.9-xi in a therapeutic setting, we began treatment 5 days post tumor challenge. The mode of treatment was also adjusted to better conform to a clinical setting by administration of the antibodies twice weekly over a period of 6 weeks. The tripling of the median survival of J22.9-xi treated animals demonstrates that this antibody is also beneficial in the treatment of established tumors. This finding was corroborated using cytokine transgenic NSG mice and delaying the start of antibody treatment to day 12.

The median survival of MM patients has increased in recent years due to improvements in treatment regimens, but MM remains incurable in most cases. New strategies for targeting the BM environment or tumor cells directly have evolved (Munshi and Anderson, 2013). Although the therapeutic use of mAbs holds promise, a multi-agent approach including mAbs might be necessary for overcoming the most difficult therapeutic challenges, such as those seen with Rituximab in the treatment of Non-Hodgkin's lymphoma (Cheson and Leonard, 2008). With J22.9-xi, we provide a new potent antibody for the treatment of MM which has comparable efficiency to the afucosylated ADC described recently (Tai et al., 2014). Further studies will need to address the efficacy and safety of antibody-based versus ADC-based approaches in curing MM in humans. The structure of the J22.9-xi Fab:BCMA complex will facilitate humanization of the variable regions while keeping the high affinity interaction intact. With this, a necessary step towards clinical development can be fulfilled.

In summary, we generated J22.9-xi, a BCMA-specific chimeric antibody showing an exceptionally high affinity receptor ligand interaction, BCMA ligand blocking capability, specific depletion of an MM cell line, and significant efficacy in preclinical tumor mouse models. Its use might not be restricted to MM, since BCMA may also be a suitable target for treating autoimmune diseases such as systemic lupus erythematosus or rheumatoid arthritis. This antibody promises to be beneficial by depleting PCs or plasma blasts producing pathogenic autoantibodies, as both highly express BCMA on their cell surface (Benson et al., 2008; Darce et al., 2007; Good et al., 2009).

Accession codes Coordinates of the BCMA-J229.xi complex have been deposited in the wwPDB database with accession code 4ZFO.

Acknowledgements

This work was supported by grants from the Helmholtz Alliance on Immunotherapy of Cancer and from The Human Frontier Science Program Organization (CDA-00007/2009-C). We would like to thank V. Schulz for technical assistance, the BESSY staff at BL14.1 and Drs. Y. Roske and K. Faelber for assistance during X ray data collection. We also thank Kerstin Krüger and Vanessa Stache for their help with the revision work.

Appendix A. Supplementary data

Supplementary data related to this article can be found at http://dx.doi.org/10.1016/j.molonc.2015.03.010.

REFERENCES

Adams, P.D., Afonine, P.V., Bunkoczi, G., Chen, V.B., Davis, I.W., Echols, N., Headd, J.J., Hung, L.W., Kapral, G.J., Grosse-Kunstleve, R.W., McCoy, A.J., Moriarty, N.W., Oeffner, R., Read, R.J., Richardson, D.C., Richardson, J.S., Terwilliger, T.C., Zwart, P.H., 2010. PHENIX: a comprehensive Python-based system for macromolecular structure solution. Acta Crystallogr. D Biol. Crystallogr. 66, 213–221.

Bellucci, R., Alyea, E.P., Chiaretti, S., Wu, C.J., Zorn, E., Weller, E., Wu, B., Canning, C., Schlossman, R., Munshi, N.C., Anderson, K.C., Ritz, J., 2005. Graft-versus-tumor response in patients with multiple myeloma is associated with antibody response to BCMA, a plasma-cell membrane receptor. Blood 105, 3945–3950.

Benson, M.J., Dillon, S.R., Castigli, E., Geha, R.S., Xu, S., Lam, K.P., Noelle, R.J., 2008. Cutting edge: the dependence of plasma cells and independence of memory B cells on BAFF and APRIL. J. Immunol. 180, 3655–3659.

Bossen, C., Schneider, P., 2006. BAFF, APRIL and their receptors: structure, function and signaling. Semin. Immunol. 18, 263–275.

Bracewell, C., Isaacs, J.D., Emery, P., Ng, W.F., 2009. Atacicept, a novel B cell-targeting biological therapy for the treatment of rheumatoid arthritis. Expert Opin. Biol. Ther. 9, 909–919.

Carpenter, R.O., Evbuomwan, M.O., Pittaluga, S., Rose, J.J., Raffeld, M., Yang, S., Gress, R.E., Hakim, F.T., Kochenderfer, J.N., 2013. B-cell maturation antigen is a promising target for adoptive T-cell therapy of multiple myeloma. Clin. Cancer Res. 19, 2048–2060.

Chen, V.B., Arendall 3rd, W.B., Headd, J.J., Keedy, D.A., Immormino, R.M., Kapral, G.J., Murray, L.W., Richardson, J.S., Richardson, D.C., 2010. MolProbity: all-atom structure validation for macromolecular crystallography. Acta Crystallogr. D Biol. Crystallogr. 66, 12–21.

Cheson, B.D., Leonard, J.P., 2008. Monoclonal antibody therapy for B-cell non-Hodgkin's lymphoma. N. Engl. J. Med. 359, 613–626.

Darce, J.R., Arendt, B.K., Wu, X., Jelinek, D.F., 2007. Regulated expression of BAFF-binding receptors during human B cell differentiation. J. Immunol. 179, 7276–7286.

Demchenko, Y.N., Glebov, O.K., Zingone, A., Keats, J.J., Bergsagel, P.L., Kuehl, W.M., 2010. Classical and/or alternative NF-kappaB pathway activation in multiple myeloma. Blood 115, 3541–3552.

Durocher, Y., Perret, S., Kamen, A., 2002. High-level and high-throughput recombinant protein production by transient transfection of suspension-growing human 293-EBNA1 cells. Nucleic Acids Res. 30, E9.

Emsley, P., Lohkamp, B., Scott, W.G., Cowtan, K., 2010. Features and development of Coot. Acta Crystallogr. D Biol. Crystallogr. 66, 486–501.

Fu, X., Tao, L., Rivera, A., Williamson, S., Song, X.T., Ahmed, N., Zhang, X., 2010. A simple and sensitive method for measuring tumor-specific T cell cytotoxicity. PLoS One 5, e11867.
Good, K.L., Avery, D.T., Tangye, S.G., 2009. Resting human memory B cells are intrinsically programmed for enhanced survival and responsiveness to diverse stimuli compared to naive B cells. J. Immunol. 182, 890–901.
Gordon, N.C., Pan, B., Hymowitz, S.G., Yin, J., Kelley, R.F., Cochran, A.G., Yan, M., Dixit, V.M., Fairbrother, W.J., Starovasnik, M.A., 2003. BAFF/BLyS receptor 3 comprises a minimal TNF receptor-like module that encodes a highly focused ligand-binding site. Biochemistry 42, 5977–5983.
Hideshima, T., Anderson, K.C., 2002. Molecular mechanisms of novel therapeutic approaches for multiple myeloma. Nat. Rev. Cancer 2, 927–937.
Hsu, J., Shi, Y., Krajewski, S., Renner, S., Fisher, M., Reed, J.C., Franke, T.F., Lichtenstein, A., 2001. The AKT kinase is activated in multiple myeloma tumor cells. Blood 98, 2853–2855.
Hymowitz, S.G., Patel, D.R., Wallweber, H.J., Runyon, S., Yan, M., Yin, J., Shriver, S.K., Gordon, N.C., Pan, B., Skelton, N.J., Kelley, R.F., Starovasnik, M.A., 2005. Structures of APRIL-receptor complexes: like BCMA, TACI employs only a single cysteine-rich domain for high affinity ligand binding. J. Biol. Chem. 280, 7218–7227.
Inki, P., Jalkanen, M., 1996. The role of syndecan-1 in malignancies. Ann. Med. 28, 63–67.
Jefferis, R., Lund, J., Pound, J.D., 1998. IgG-Fc-mediated effector functions: molecular definition of interaction sites for effector ligands and the role of glycosylation. Immunol. Rev. 163, 59–76.
Kabsch, W., 2010. Xds. Acta Crystallogr. D Biol. Crystallogr. 66, 125–132.
Laskowski, R.A., Hutchinson, E.G., Michie, A.D., Wallace, A.C., Jones, M.L., Thornton, J.M., 1997. PDBsum: a web-based database of summaries and analyses of all PDB structures. Trends Biochem. Sci. 22, 488–490.
Liu, Y., Hong, X., Kappler, J., Jiang, L., Zhang, R., Xu, L., Pan, C.H., Martin, W.E., Murphy, R.C., Shu, H.B., Dai, S., Zhang, G., 2003. Ligand-receptor binding revealed by the TNF family member TALL-1. Nature 423, 49–56.
Mackay, F., Schneider, P., Rennert, P., Browning, J., 2003. BAFF AND APRIL: a tutorial on B cell survival. Annu. Rev. Immunol. 21, 231–264.
Malavasi, F., Deaglio, S., Funaro, A., Ferrero, E., Horenstein, A.L., Ortolan, E., Vaisitti, T., Aydin, S., 2008. Evolution and function of the ADP ribosyl cyclase/CD38 gene family in physiology and pathology. Physiol. Rev. 88, 841–886.
Meyer, T.P., Zehnter, I., Hofmann, B., Zaisserer, J., Burkhart, J., Rapp, S., Weinauer, F., Schmitz, J., Illert, W.E., 2005. Filter Buffy Coats (FBC): a source of peripheral blood leukocytes recovered from leukocyte depletion filters. J. Immunol. Methods 307, 150–166.
Munshi, N.C., Anderson, K.C., 2013. New strategies in the treatment of multiple myeloma. Clin. Cancer Res. 19 (13), 3337–3344.
Nezlin, R., Ghetie, V., 2004. Interactions of immunoglobulins outside the antigen-combining site. Adv. Immunol. 82, 155–215.
Nimmerjahn F. and Ravetch J.V., Fcg receptors as regulators of immune responses, Nat. Rev. Immunol., 8, 34–47, doi:10.1038/nri2206
Novak, A.J., Darce, J.R., Arendt, B.K., Harder, B., Henderson, K., Kindsvogel, W., Gross, J.A., Greipp, P.R., Jelinek, D.F., 2004. Expression of BCMA, TACI, and BAFF-R in multiple myeloma: a mechanism for growth and survival. Blood 103, 689–694.
O'Connor, B.P., Raman, V.S., Erickson, L.D., Cook, W.J., Weaver, L.K., Ahonen, C., Lin, L.L., Mantchev, G.T., Bram, R.J., Noelle, R.J., 2004. BCMA is essential for the survival of long-lived bone marrow plasma cells. J. Exp. Med. 199, 91–98.
Palumbo, A., Anderson, K., 2011. Multiple myeloma. N. Engl. J. Med. 364, 1046–1060.
Peperzak, V., Vikstrom, I., Walker, J., Glaser, S.P., Lepage, M., Coquery, C.M., Erickson, L.D., Fairfax, K., Mackay, F., Strasser, A., Nutt, S.L., Tarlinton, D.M., 2013. Mcl-1 is essential for the survival of plasma cells. Nat. Immunol.. http://dx.doi.org/10.1038/ni.2527
Raab, M.S., Podar, K., Breitkreutz, I., Richardson, P.G., Anderson, K.C., 2009. Multiple myeloma. Lancet 374, 324–339.
Ramakrishnan, V., Kimlinger, T., Haug, J., Painuly, U., Wellik, L., Halling, T., Rajkumar, S.V., Kumar, S., 2012. Anti-Myeloma activity of Akt inhibition linked to the activation status of PI3K/Akt and MEK/ERK pathway. PLoS One 7, e50005.
Richardson, P.G., Barlogie, B., Berenson, J., Singhal, S., Jagannath, S., Irwin, D., Rajkumar, S.V., Srkalovic, G., Alsina, M., Alexanian, R., Siegel, D., Orlowski, R.Z., Kuter, D., Limentani, S.A., Lee, S., Hideshima, T., Esseltine, D.L., Kauffman, M., Adams, J., Schenkein, D.P., Anderson, K.C., 2003. A phase 2 study of bortezomib in relapsed, refractory myeloma. N. Engl. J. Med. 348, 2609–2617.
Rickert, R.C., Jellusova, J., Miletic, A.V., 2011. Signaling by the tumor necrosis factor receptor superfamily in B-cell biology and disease. Immunol. Rev. 244, 115–133.
Rossi, J.F., Moreaux, J., Hose, D., Requirand, G., Rose, M., Rouille, V., Nestorov, I., Mordenti, G., Goldschmidt, H., Ythier, A., Klein, B., 2009. Atacicept in relapsed/refractory multiple myeloma or active Waldenstrom's macroglobulinemia: a phase I study. Br. J. Cancer 101, 1051–1058.
Ryan, M.C., Hering, M., Peckham, D., McDonagh, C.F., Brown, L., Kim, K.M., Meyer, D.L., Zabinski, R.F., Grewal, I.S., Carter, P.J., 2007. Antibody targeting of B-cell maturation antigen on malignant plasma cells. Mol. Cancer Ther. 6, 3009–3018.
Schwartz, R.N., Vozniak, M., 2008. Current and emerging treatments for multiple myeloma. J. Manag. Care Pharm. : JMCP 14, 12–19.
Shields, R.L., Namenuk, A.K., Hong, K., Meng, Y.G., Rae, J., Briggs, J., Xie, D., Lai, J., Stadlen, A., Li, B., Fox, J.A., Presta, L.G., 2001. High resolution mapping of the binding site on human IgG1 for Fc gamma RI, Fc gamma RII, Fc gamma RIII, and FcRn and design of IgG1 variants with improved binding to the Fc gamma R. J. Biol. Chem. 276, 6591–6604.
Tai, Y.T., Anderson, K.C., 2011. Antibody-based therapies in multiple myeloma. Bone Marrow Res. 2011, 924058.
Tai, Y.T., Mayes, P.A., Acharya, C., Zhong, M.Y., Cea, M., Cagnetta, A., Craigen, J., Yates, J., Gliddon, L., Fieles, W., Hoang, B., Tunstead, J., Christie, A.L., Kung, A.L., Richardson, P., Munshi, N.C., Anderson, K.C., 2014. Novel afucosylated anti-B cell maturation antigen-monomethyl auristatin F antibody-drug conjugate (GSK2857916) induces potent and selective anti-multiple myeloma activity. Blood 23 (20), 3128–3138.
Tiller, T., Busse, C.E., Wardemann, H., 2009. Cloning and expression of murine Ig genes from single B cells. J. Immunol. Methods 350, 183–193.
Vagin, A., Teplyakov, A., 2010. Molecular replacement with MOLREP. Acta Crystallogr. D Biol. Crystallogr. 66, 22–25.
Xu, X.J., Tang, Y.M., 2014. Cytokine release syndrome in cancer immunotherapy with chimeric antigen receptor engineered T cells. Cancer Lett. 343, 172–178.
Yang, J., Yi, Q., 2011. Therapeutic monoclonal antibodies for multiple myeloma: an update and future perspectives. Am. J. Blood Res. 1, 22–33.
Yokoyama, W.M., 2006. Production of monoclonal antibodies. Curr. Protoc. Cytom. Appendix 3, Appendix 3j.